Bowel stiffness associated with histopathologic scoring of stenosis in patients with Crohn's disease

Zhao, Jingbo; Liao, Donghua; Wilkens, Rune; Krogh, Klaus; Glerup, Henning; Gregersen, Hans

Published in:
Acta Biomaterialia

DOI (link to publication from Publisher):
10.1016/j.actbio.2021.06.011

Publication date:
2021

Document Version
Publisher's PDF, also known as Version of record

Acta Biomaterialia 130 (2021) 332–342

Contents lists available at ScienceDirect

Acta Biomaterialia

journal homepage: www.elsevier.com/locate/actbio

Full length article

Bowel stiffness associated with histopathologic scoring of stenosis in patients with Crohn's disease

Jingbo Zhao[a,b,c], Donghua Liao[b,c,*], Rune Wilkens[d,e], Klaus Krogh[f], Henning Glerup[e], Hans Gregersen[g]

[a] Standard (Chongqing) Pathological Diagnosis Center. No. 8 Xiyuan North Road, Shapingba District, Chongqing, China
[b] Mech-Sense, Department of Gastroenterology and Hepatology, Aalborg University Hospital, Denmark
[c] Giome Academia, Department of Clinical Medicine, Aarhus University, Aarhus, Denmark
[d] Gastrounit, Division of Medicine, Hvidovre Hospital, University of Copenhagen, Copenhagen, Denmark
[e] Diagnostic Centre, University Research Clinic for Innovative Patient Pathways, Silkeborg Regional Hospital, Silkeborg, Denmark
[f] Neurogastroenterology Unit, Department of Hepatology and Gastroenterology, Aarhus University Hospital, Aarhus, Denmark
[g] GIOME, Calmi2, San Diego, California, USA

ARTICLE INFO

Article history:
Received 26 January 2021
Revised 31 May 2021
Accepted 3 June 2021
Available online 10 June 2021

Keywords:
Crohn's disease
Stenotic site
Stiffness
Fibrosis
Chronic inflammation

ABSTRACT

Background and aims: Intestinal stenosis is a common complication of Crohn's Disease (CD). Stenosis is associated with alteration of bowel mechanical properties. This study aims to quantitate the mechanical properties of the intestinal stenosis and to explore associations between histology and mechanical remodeling at stenotic intestinal sites in CD patients. *Methods*: Intestinal segments from stenotic sites were studied in vitro from 19 CD patients. A luminal catheter with a bag was used to stepwise pressurize the intestinal segments from 0-100 cmH_2O with 10 cmH_2O increments. B-mode ultrasound images were obtained at the narrowest part of the stenosis at each pressure level and morphometric parameters were obtained from ultrasound images. The mechanical behavior of the stenotic tissue were characterized by using an isotropic three dimensional strain energy function in Demiray model form, the mechanical constants were obtained by fitting the model to the recorded intraluminal pressure and the inner radius of the stenotic segment of the small bowel. Grading scores were used for histological analysis of inflammation, fibrosis, muscular hypertrophy and adipocyte proliferation in the intestinal layers. The collagen area fraction in intestinal layers was also calculated. Associations between histological and the mechanical constants (stiffness) were analyzed. *Results*: Chronic inflammation was mainly located in mucosa whereas fibrosis was found in submucosa. The mechanical remodeling was performed with changed mechanical constants ranged between 0.35-13.68kPa. The mechanical properties changes were associated mainly with chronic inflammation, fibrosis and combination of inflammation and fibrosis ($R>0.69$, $P<0.001$). Furthermore, the mechanical properties correlated with the collagen fraction in submucosa and muscular layers ($R>0.53$, $P<0.05$). *Conclusions*: We quantitated the intestinal stenosis stiffness. Associations were found between bowel mechanical remodeling and histological changes at the stenotic site in CD patients.

Statement of significance

Although intestinal ultrasonography, CT and MRI can be used to diagnose Crohn's Disease (CD)-associated bowel strictures, these techniques may not have sufficient accuracy and resolution to differentiate predominantly inflammatory strictures from predominantly fibrotic strictures. The present study aims to quantitate the mechanical remodeling of intestinal stenosis and to explore the associations between histological parameters and mechanical properties at the intestinal stenotic sites in CD patients. For the first time, we quantitatively demonstrated that the mechanical properties of the intestinal wall in CD stenosis

* Corresponding author at: Mech-Sense, Department of Gastroenterology and Hepatology, Aalborg University Hospital, Aalborg, Denmark.
E-mail address: dl@rn.dk (D. Liao).

https://doi.org/10.1016/j.actbio.2021.06.011

are associated with the chronic inflammation, fibrosis and collagen fraction in the intestinal layers. The results of this study may facilitate design and development of artificial biomaterials for gastrointestinal organs. The potential clinical implication of this study is that the histological characteristics in patients with CD can be predicted clinically by means of inflammation and fibrosis assessment in conjunction with tissue stiffness measurement.

1. Introduction

Crohnś disease (CD) is a chronic, relapsing inflammatory bowel disease (IBD) that affect various parts of the gastrointestinal tract, most commonly the small intestine and colon [1,2]. The incidence of CD ranges from 5 to 30 cases per 100,000 person-years in Western countries [3]. Symptoms usually include diarrhea, abdominal pain, rectal bleeding, fever, weight loss, or fatigue [1,2]. Common complications of the chronic transmural inflammation in CD are fistulae, abscesses, intestinal perforation, and intestinal strictures [4].

Chronic inflammation, ulcerations, and injury to the intestinal wall may lead to disorganized deposition of extracellular matrix [5]. Moreover, due to the transmural inflammation in CD, fibrosis may involve all layers of the bowel wall. This results in wall thickening and stiffening with narrowing of the intestinal lumen, leading to strictures and obstruction [5]. Chen and co-workers developed a comprehensive analysis of the histopathological elements in CD [6]. Their histological grading system covers not only inflammation and fibrosis but the full spectrum of histopathology in IBD.

Although intestinal ultrasonography, CT and MRI can be used to diagnose CD-associated bowel strictures [7], these techniques may not have sufficient accuracy and resolution to differentiate predominantly inflammatory strictures from predominantly fibrotic strictures. Intestinal ultrasonography and contrast enhanced ultrasonography may be useful for assessment of bowel stiffness and inflammation, i.e. to differentiate between acute bowel wall inflammation, fibrosis, and muscularization [8]. However, these modalities are still experimental, and the stiffness measurements are difficult to compare with traditional engineering quantifications of soft tissue stiffness [9]. It has been shown that bowel wall stiffness increased in regions with fibrotic changes [10-12]. The study from Johnson et al showed that the matrix stiffness activates human colonic fibroblasts to a fibrogenic phenotype [12]. It suggests the mechanical properties of the cellular environment are critical to fibroblast function. Hence, the changes in mechanical properties (stiffness) in CD-associated stenosis is likely important for understanding mechanisms for intestinal fibrosis. The aims of the present study were to quantitate the mechanical remodeling of intestinal stenosis and to explore the associations between histological parameters and mechanical properties change at the intestinal stenotic sites in CD patients. We hypothesized that associations exist between intestinal mechanical properties and CD-induced inflammation and fibrosis. The potential clinical implication of this study is that in vivo stiffness measurements can be used to predict developments of the histological stenosis characteristics of the small bowel in CD.

2. Material and methods

Inclusion criteria were CD patients referred to elective surgery for small intestinal disease regardless of activity. Twenty-five patients (mean age, 37 years; range 19-67 years; 12 females) were recruited for the study during September 2012 to March 2014 in Denmark. Bag distension was not done in excised intestine from six of the patients due to lack of time, technical failure, and missing data (two in each category). Consequently, excised intestines from 19 patients were included in the present study. Patients reported symptoms including pain, vomiting, diarrhea, and bloating and Crohn's disease activity index (CDAI) were calculated. Supplemental Table S1 shows CDAI and the symptom scores for the patients and supplemental Table S2 shows preoperative imaging parameters of the surgical specimens. Results for preoperative cross-sectional imaging findings and simple histology have been published [13].

2.1. Ethics statement

All procedures followed were in accordance with the ethical standards of the responsible committee on human experimentation (institutional and national) and with the Helsinki Declaration of 1975, as revised in 2008. Informed consent was obtained from all patients for being included in the study. The study was approved by the municipality IEB (approval 1-10-72-339-12) and Danish national authorities (ID number of EudraCT=2011-005846-36).

2.2. Tissue sampling and biomechanical testing

Tissue sampling and testing have been described previously [13]. Immediately after surgical excision, the bowel segment was rinsed with tab water and fixated at the in vivo length (measured during surgery) in an organ bath. The organ bath contained standard Krebs solution with glucose and ascorbic acid at 37°C [14]. The temperature was maintained constant using an electric warming tray (Bartscher, Salzkotten, Germany). A 3mm-diameter-catheter with a bag that could be distended to diameter 30mm without stretching the bag was connected to a water column system used for distension of the tissue segment. The size of the bag ensured that the applied bag pressure was fully transmitted to the intestinal wall at the stricture site. The distension pressure was subsequently increased up to 100 cmH_2O in steps of 10 cmH_2O. Ultrasound b-mode images of the specimen in cross-section were obtained at the narrowest part of the stenosis after obtaining pressure equilibrium at each step (HI VISION Preirus US machine with a EUP-L73S probe. Hitachi Medical Corporation, Tokyo). Images were exported in DICOM format.

The pressure imposed by the bag distension and the ultrasound images at each pressure level were used for the biomechanical analyses.

2.3. Ultrasound image analysis

US DICOM images were analyzed using radiology imaging software, OsiriX 5.7.1. 64 bit (Pixmeo SARL, Bernex, Switzerland). A circular/ovoid region of interest (ROI) was drawn for the luminal border and the outer muscularis propria border of the bowel wall and were annotated according to location and pressure level (Supplemental Fig. S3) [13]. ROIs from all pressure levels containing information about area and circumference were exported in csv format and imported into MATLAB (R2020, The MathWorks Inc.) for further analysis, see below.

2.4. Biomechanical data analysis

The stenotic segment of the small bowel was assumed to be a thick-walled tube made of nonlinear hyperelastic, incompressible, isotropic and homogeneous material. The viscoelasticity, the active behavior of the small bowel, and anisotropy were not considered. The small bowel model is described in cylindrical coordinates with (θ, r and z) as the orientations in circumferential, radial and longitudinal directions. The deformation field in the mechanical testing is described from a unloaded configuration *X (R, Θ, Z)* to pressurized configuration *x (r,θ,z)* with relationship:

$$r = r(R), \theta = \Theta, z = \lambda_z Z \tag{1}$$

where *X (R, Θ, Z),* and *x (r,θ,z)* are the reference and current pressurized position of a material particle, and λ_z is the distension induced axial stretch. The deformation of the model is described in terms of the deformation gradient as:

$$\mathbf{F} = \frac{\partial x}{\partial X} = diag\left[\frac{\partial r}{\partial R}, \frac{r}{R}, \frac{z}{Z}\right] = diag[\lambda_r, \lambda_\theta, \lambda_z] \tag{2}$$

where $\lambda_r, \lambda_\theta, \lambda_z$ are stretches in radial, circumferential and axial directions.

Circumference and luminal areas for the inner surface and outer surface of the narrowest part of the stenosis were measured from the US images. The inner radius (r_{ip}) outer radius (r_{op}), λ_θ, λ_r and λ_z at each distension pressure at the narrowest stenosis location were calculated as:

$$r_{ip} = \sqrt{LA_{ip}/\pi} \tag{3}$$

$$r_{op} = \sqrt{LA_{op}/\pi} \tag{4}$$

$$\lambda_\theta = r/R$$

$$\lambda_r = \frac{dr}{dR} = 1/(\lambda_\theta \lambda_z) \tag{5}$$

$$\lambda_z = (R_o^2 - R_i^2)/(r_{op}^2 - r_{ip}^2) = \ f\left(r_{ip}\right) \tag{6}$$

where LA_{ip},LA_{op}, r_{ip},r_{op} are luminal area and radius for inner and outer surfaces, the subscript p = 0, 10, 20, …100 indicates the distension pressure from 0 to 100 cmH_2O, R_i, R_o are inner and outer radius at pressure = 0. $f(r_{ip})$ is λ_z change over the distension, in this study, $f(r_{ip}) = C(\frac{r_{ip}}{R_i} - 1) + 1$ was used, and the constant C was obtained by curve fitting the r_{ip}/R_i to the λ_z change over the distensions for all tests.

The small bowel tissue was assumed incompressible, consequently:

$$\lambda_r \lambda_\theta \lambda_z = 1 \tag{7}$$

From Eq. (7), the radius along the small bowel at the reference state (R) can be expressed as a function of the radius in the loaded state (r) as:

$$R = \sqrt{\lambda_z * \left(r^2 - {r_{ip}}^2\right) + {R_i}^2} \tag{8}$$

R_i is the inner radius of the small bowel at the reference state.

The mechanical behavior of the small bowel segment was characterized by an isotropic three-dimensional strain energy function in Demiray model form as [15,16]:

$$W = \frac{a}{b}\left[exp\left(\frac{b}{2}(I_1 - 3)\right) - 1\right] \tag{9}$$

where a and b are positive constants, a represents the shear modulus of the material and b is a positive dimensionless material parameter, which represents the degree of material nonlinearity. $I_1 = tr\mathbf{C}$ is the first invariants of the strain tensor and $\mathbf{C} = \mathbf{F}^T\mathbf{F}$. In this study, the parameter $AB = a^*b$ was used for the association analysis between the mechanical properties and the histological characteristics.

The associated Cauchy stress σ is given by:

$$\sigma = -p\mathbf{I} + 2\mathbf{F}\frac{\partial W}{\partial \mathbf{C}}\mathbf{F}^T \tag{10}$$

where p is a Lagrange multiplier associated with the constraint and represents a contribution to the hydrostatic stress, and $\mathbf{I}$ is the identity tensor.

The second term on the right side of Eq. 7 can be written as:

$$\sigma^p = 2\boldsymbol{F}\frac{\partial W}{\partial \boldsymbol{C}}\boldsymbol{F}^T = 2W_1\boldsymbol{B} \tag{11}$$

where $\mathbf{B} = \mathbf{F}\mathbf{F}^T$, $W_1 = \partial W/\partial I_1$,

The component of the Cauchy stresses are:

$$\sigma_{rr} = -p + a.exp\left(\frac{b}{2}(I_1 - 3)\right).{\lambda_r}^2$$

$$\sigma_{\theta\theta} = -p + a.exp\left(\frac{b}{2}(I_1 - 3)\right).{\lambda_\theta}^2$$

$$\sigma_{zz} = -p + a.exp\left(\frac{b}{2}(I_1 - 3)\right).{\lambda_z}^2 \tag{12}$$

Due to the symmetry, there is no shear stress and the normal stresses σ_{rr}, $\sigma_{\theta\theta}$ and σ_{zz} are principal stresses. The equilibrium equation consists of just the radial equation, i.e.

$$\frac{d\sigma_{rr}}{dr} + \frac{\sigma_{rr} - \sigma_{\theta\theta}}{r} = 0 \tag{13}$$

Eq. 13 can be solved by integrating over radius from the inner wall (r_i) to the outer surface (r_o) as:

$$\sigma_{rr}(r_o) - \sigma_{rr}(r_i) = -\int_{r_i}^{r_o} \frac{\sigma_{rr} - \sigma_{\theta\theta}}{r} dr \tag{14}$$

Integration of Eq. 14 and application of the boundary conditions $\sigma_{rr} = -P(t)$ on $r = r_i$ and $\sigma_{rr} = 0$ on $r = r_o$, leads to the expression:

$$P(t) = \int_{r_{ip}}^{r_{op}} \frac{(\sigma_{\theta\theta}(r,t) - \sigma_{rr}(r,t))}{r} dr \tag{15}$$

where $P(t)$ is the calculated intraluminal pressure at the loading state.

The intraluminal pressure $P(t)$ in Eq. 15 is a function of material constants A (a,b), longitudinal stretch ratio λ_z, and inner radius of the segment. They can be expressed by J_p as [17,18]:

$$P(t) = J_p\left(A, \lambda_z, r_{ip}\right) \tag{16}$$

where J_p is:

$$J_p = \int_{r_{ip}}^{r_{op}} \frac{1}{r}\ a.\exp\left(\tfrac{b}{2}.(I_1 - 3)\right).\quad \left({\lambda_\theta}^2 - {\lambda_r}^2\right)dr \tag{17}$$

where $I_1 = ({\lambda_r}^2 + {\lambda_\theta}^2 + {\lambda_z}^2)$, $r_{op} = \sqrt{\frac{1}{\lambda_z}(R_o^2 - R_i^2) + {r_{ip}}^2}$, where R_o is the outer radius of the segment at the reference state.

Best-fit values of these parameters were determined using a nonlinear least-squares (Levenberg-Marquardt) minimization of the difference between computed and measured intraluminal pressures during the distension. The integral function in Eq. 14 is numerically approximated by using Romberg's method, i.e., the following objective function was minimized:

$$S(A) = \sum_{i=1}^{m} [J_p(A, \lambda_2, r_i) - p_i]^2 \tag{18}$$

where m is the number of data points, J_p the computed intraluminal pressure from (17), and p_i the measured bag pressure. The unknown material parameters a and b were obtained by fitting the model to the recorded intraluminal pressure- inner radius curves of the stenotic segment of the small bowel. As a metric of the goodness of fit, we computed the root mean square of the fitting error:

$$RMSE = \sqrt{\frac{S(A)}{m}} \tag{19}$$

All calculations were optimized by using MATLAB subroutines (R2020, Mathworks, USA).

2.5. Tissue sampling for histology

Tissue sampling for histology has been described in detail previously [13]. To preserve the original shape and luminal diameter, the bowel segment was not opened longitudinally. Fixation was made in neutral buffered formaldehyde for 24-48 hours using intraluminal wicks to ensure sufficient preservation. After fixation, all segments were transversally cut into slices of 3-6 mm thickness (Supplementary Fig. S4). The whole mounted slices were then paraffin-embedded for sectioning. The slices were stained with 1) Haematoxylin-eosin (HE), 2) Masson's trichrome (Masson), and 3) anti-Desmin, respectively. Slices were digitalized with NanoZoomer 2.0 HT and NanoZoomer 2.0-RS (Hamamatsu, Hamamatsu City, Japan).

2.6. Grading of inflammation, fibrosis, muscular hypertrophy and adipocyte proliferation

In order to evaluate the degree of histological remodeling in the CD stenosis, we adopted the method proposed by Chen et al [6] with minor modifications. As we did not have histological slides from "normal locations" of the CD bowel, the "space volume (thickness) expansion" in different layers could not be graded. Furthermore, we did not analyze the neuronal hypertrophy parameter. We scored 0, 1, 2 and 3 for the degrees of specific changes in each layer of the CD stenosis as inflammation score, fibrosis score, muscular hyperplasia score and adipocyte proliferation score (Supplemental Table S5-8). HE stained slides were used to evaluate acute and chronic inflammations (Supplemental Table S5) and adipocyte proliferation (Supplemental Table S8), Masson stained slides for fibrosis/collagen expression (Supplemental Table S6), and anti-Desmin stained slides for muscular hypertrophy (Supplemental Table S7). The scores of adipocyte proliferation was only evaluated in submucosa and muscle layers. The degree of fibrosis in various layers was evaluated in two different ways; an ordinal score from 0 to 3 and a relative measure of collagen in submucosa and muscle layers, calculated from the collagen and the total wall areas from Masson stained slides (Fig. 1). All calculations were done by using a house made MATLAB subroutine (R2020, MathWorks Inc.). The total scores of each histological parameter in the intact wall were obtained by summation of histological scores in the layers.

2.7. Association analyses between histological parameters and stiffness of the CD stenosis and statistical analyses

The histological parameters and the mechanical properties of the CD stenosis were analyzed independently by observers blinded to each other's findings. The combined material constant AB = a*b in Eq. 9 were used for describing the stiffness of the wall. The relationships between histological scores and the stiffness of the CD stenosis were analyzed using:

1) multiple linear regression analysis to identify the dominant histological factors of the intact wall that related to the stiffness.

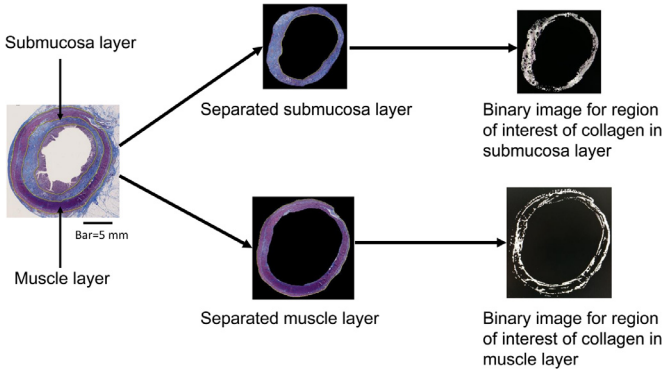

Fig. 1. Method for measurement of the collagen fraction in submucosa and muscle layers. First, submucosa and muscle layers were outlined and separated into two images. Second, the region of interest (ROI) of collagen in Masson stained slides was defined by using image segmentation method. Third, the color due to collagen was distinguished in the ROI using intensity thresholds. Finally, the images were exported as binary images and the area fraction of collagen was calculated.

2) single linear regression analysis to analyze the association between the dominant histological factors and the stiffness.
3) multiple linear analysis again to identify the layers contribution of the dominant histological factors to the stiffness.
4) single linear regression analysis to analyze the associations between collagen fraction and the stiffness.

During the association analysis, correlation coefficients R was used to determine correlations between variables, F and P were F-test value and P-value for the F-test, and a P-value of <0.05 was considered significance for all analyses. In multiple linear regression analysis, the dependent variable can be predicted from linear combination of the independent variables, and the smaller P-value of the independent variables indicated its closer relation with the dependent variable. Data are presented as mean±SD, and all analyses were computed using SigmaPlot version 11.0 (Systat Software, Inc.).

3. Results

Data from 19 CD patients were included. Supplemental Table S1 shows the patients demographical data including age (43.4 ± 13.4 years, range 19-67 years), gender (11/8 F/M), BMI (24.9 ± 3.5), duration of disease (5 cases < 2 years, 7 cases 2-10 years and 7 cases >10 years), CDAI (200.3± 99.1) and symptoms (pain, vomiting, diarrhea, and bloating, detail scores are shown in Supplemental Table S1).

3.1. Histological grading/scores

Representative examples of intact wall slices with histological scores are shown in Fig. 2. The scores from each segment and average scores of all segments for acute and chronic inflammation, fibrosis, muscle hypertrophy and adipocyte deposition in different layers and summation of the scores are listed in Table 1. The highest average score for acute and chronic inflammation was in the mucosa. Fibrosis and adipocyte deposition were primarily in submucosa.

3.2. Mechanical properties of the tissue

The inner diameter at the stenotic site at the maximum distension pressure was 16.4±6.7 mm (ranging from 7.4 to 27.8mm). The mechanical constants (a and b) in Eq. 9 were calculated by curve fitting Eq. 17 to the recorded intraluminal pressure-inner radius data. The fitted mechanical constants and residuals are listed in

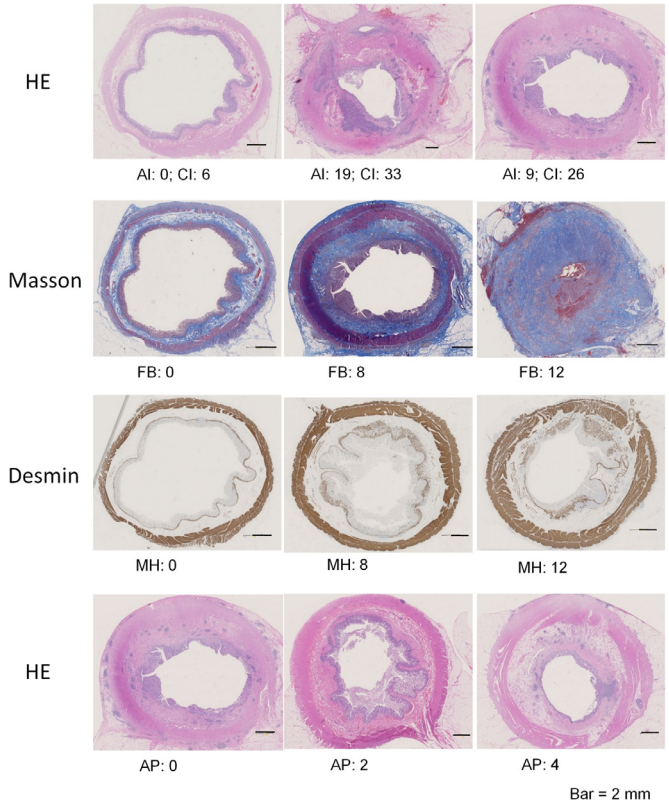

Fig. 2. Examples of histological scores obtained from the intact wall. The first row is scores for inflammation including acute and chronic, the second row for fibrosis, the third row for muscular hypertrophy, and the last row for adipocyte proliferation. The scores from low to high indicating the severity of the histological changes. Acute inflammation was considered by fissuring ulcer involvement, abscess, polymorphonuclear cell infiltration in non-ulcer/abscess area in the layers. For the mucosal layer superficial ulcer and cryptitis were also considered as acute inflammation. Chronic inflammation was described in terms of lymphoplasmacytic infiltration, eosinophilic infiltration and lymphoid follicles/aggregates in the various layers. In the mucosa, alteration of crypt architecture was also regarded as chronic changes. Muscular hypertrophy evaluation included lamina propria smooth muscle bundle dissection and muscularis mucosae thickening in mucosa layer, smooth muscle bundle proliferation and muscularis mucosae downward dissection in submucosa layer, and thickening of muscularis propria. Abbreviations: HE, hematoxylin and eosin staining; Masson, Masson's trichrome staining; Desmin, anti-desmin staining; AI, acute inflammation; CI, chronic inflammation; FB, fibrosis; MH, muscle hypertrophy; AP, adipocyte proliferation

Table 2. Two representative curve fittings from two patients with chronic inflammation and fibrosis scores of 19 and 42 are shown in Figure 3. The fitted curves agreed well with the recorded data, indicating the selected Demiray-type strain energy function model was valid for description of the mechanical bowel remodeling in CD patients.

3.3. Dominant histological factors determining the stiffness in the intact wall

Multiple linear regression analyses showed that the combined material constant AB was primarily associated with chronic inflammation and fibrosis (Table 3). The association between the material constant with acute + chronic inflammation, chronic inflammation + fibrosis, and scores of all factors showed that AB was primarily determined by chronic inflammation + fibrosis. Multiple linear regression equations for independent variables are presented in Table 3.

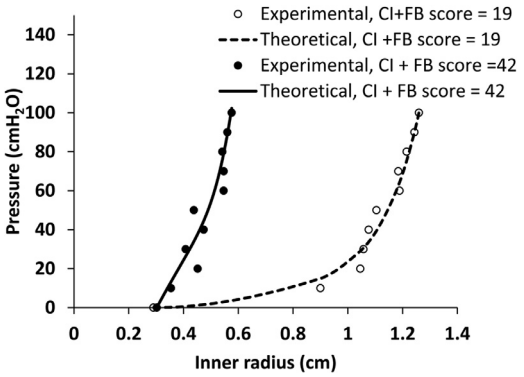

Fig. 3. Comparison of the recorded pressure-inner radius curves with the theoretical curves predicted from Eq. 16. The dashed line is from a patient with a low chronic inflammation + fibrosis score (19), and the solid line is from a patient with a high chronic inflammation + fibrosis scores (42). CI: Chronic inflammation, and FB: Fibrosis.

3.4. Associations between the stiffness and each dominant histological factor from the intact wall

Associations between AB and main histological scores are displayed in Fig. 4. It confirmed the positive associations between the AB and chronic inflammation (R=0.69, P<0.001), fibrosis (R=0.73, P<0.001) and chronic inflammation + fibrosis (R=0.74, P<0.001).

3.5. Associations between the stiffness and collagen fraction

Fig. 5 shows linear regression analysis between AB and collagen fractions in muscle and submucosa layers. The AB was associated with submucosa collagen fraction (Fig. 5a, $R = 0.53$, $P = 0.019$) and muscular collagen fraction (Fig. 5B, $R = 0.60$, $P = 0.007$).

3.6. Associations between stiffness and dominant histological factors in the layers

Table 3 shows multiple linear regression analysis assessing associations between AB and each histological component in individual bowel layers. The AB was primarily associated with chronic inflammation in mucosa layer, fibrosis in submucosa and muscle layers, and chronic inflammation + fibrosis in both mucosa and submucosa layers.

4. Discussion

4.1. Summary of the results

To the best of our knowledge, this is the first study that present detailed and quantitative stiffness analyses of intestinal stenosis in CD. Furthermore, correlation analyses between the stiffness and CD induced histological changes in the stenosis location showed: 1) the intestinal wall stiffness of CD stenosis was primarily associated with chronic inflammation of the mucosa, fibrosis in submucosa and muscle, and a combination of these two factors in mucosa and submucosa, and 2) the combined material constant was associated with the submucosal and muscle collagen fraction.

Mechanical remodeling induced by diseases in the gastrointestinal tract have been studied clinically to some extent by means of distension technologies including impedance planimetry and the functional luminal imaging probe (FLIP) [19-27]. Stiffness parameters such as the elastic modulus, compliance and distensibility index have been used as potential biomarkers of impaired gastrointestinal function [9,23]. In this study, we moved a step further by linking the remodeled mechanical properties to pathologi-

Table 1
Histological grading/scoring of strictures.

Patient No.		3	4	7	8	9	10	11	12	13	15	16	17	18	19	20	22	23	24	25	Average
Muc	AI	10	7	10	5	5	4	6	8	2	5	0	5	10	7	7	8	9	11	1	6.32
	CI	11	8	11	7	10	9	5	9	4	12	5	8	6	7	8	12	10	12	7	8.47
	FB	2	3	2	1	1	2	2	1	1	3	0	1	1	2	2	3	3	2	3	1.84
	MH	3	5	5	3	4	2	5	5	3	6	0	5	6	4	4	6	5	5	6	4.32
Sub	AI	6	1	2	1	0	0	2	1	0	0	0	1	4	2	4	6	2	1	0	1.74
	CI	4	4	6	5	8	7	7	7	4	7	1	5	4	7	7	9	8	7	4	5.84
	FB	1	1	3	1	3	3	2	3	1	2	0	2	3	1	2	3	3	3	3	2.11
	MH	1	1	1	1	2	2	3	3	1	3	0	2	4	1	1	5	3	2	6	2.21
	Adipo	3	3	2	2	0	1	0	1	2	3	3	1	2	3	2	2	1	3	2	1.89
Mus	AI	3	0	0	0	0	0	1	1	0	2	0	0	3	0	2	3	1	0	0	0.84
	CI	3	1	4	4	7	5	6	3	1	7	0	1	5	5	6	9	4	3	4	4.11
	FB	1	1	2	1	3	3	2	1	0	3	0	1	2	1	2	3	2	1	3	1.68
	MH	2	0	3	0	4	6	2	2	2	5	0	1	5	1	1	3	3	3	3	2.53
	Adipo	1	1	0	1	0	0	0	0	0	1	0	0	0	1	1	0	1	1	1	0.47
Adv	AI	2	0	0	0	0	0	0	0	0	1	0	0	0	2	1	3	1	1	0	0.58
	CI	5	1	4	5	7	7	7	7	2	7	0	2	1	6	5	9	7	4	3	4.68
	FB	2	0	2	1	2	3	3	3	0	1	0	1	1	2	1	3	1	0	1	1.47
	MH	0	0	1	0	0	1	1	1	0	1	0	2	1	0	0	2	3	0	2	0.79
Tot	AI	21	8	12	6	5	4	9	10	2	8	0	6	17	11	14	20	13	13	1	9.47
	CI	23	14	25	21	32	28	25	26	11	33	6	16	16	25	26	39	29	16	18	23.1
	FB	6	5	9	4	9	11	9	8	2	9	0	5	7	6	7	12	9	6	11	7.11
	MH	6	6	10	4	10	11	11	11	6	15	0	10	16	6	6	16	14	10	19	9.84
	Adipo	4	4	2	3	0	1	0	1	2	4	3	1	2	4	3	2	2	4	3	2.37

Notes: Adipo: Adipocyte deposition; Adv: adventitial layer; AI: acute inflammation; CI: chronic inflammation; FB: fibrosis; MH: muscle hypertrophy; Muc: mucosa; Mus: muscle; Sub: submucosa; Tot: cumulative changes of whole wall.

Table 2
Best-fitted mechanical constants at CD induced stenotic site of the small bowel.

Patient No.	a	b	AB	RSME	c
3	3.35	1.15	3.84	0.30	0.02
4	0.59	0.59	0.35	0.50	0.08
7	20.58	0.50	10.32	0.50	0.13
8	0.63	1.11	0.71	0.25	0.19
9	5.39	2.14	11.53	0.25	0.29
10	6.90	1.52	10.49	0.74	0.41
11	3.35	1.15	3.84	1.40	0.28
12	0.77	5.00	3.85	0.68	0.67
13	1.02	1.84	1.87	0.44	0.22
15	3.15	4.34	13.68	0.33	0.29
16	2.05	0.81	1.67	0.43	0.10
17	0.89	0.82	0.72	0.98	0.01
18	2.25	0.84	1.89	0.25	0.07
19	0.94	1.20	1.13	0.66	0.01
20	4.46	0.62	2.75	0.36	0.15
22	2.69	3.91	10.53	0.67	0.09
23	3.17	2.05	6.49	0.27	0.19
24	5.95	0.86	5.14	0.75	1.47
25	17.56	0.50	8.85	0.17	0.29

Notes: a,b, AB= a^*b are mechanical constants in Eq. 9. RMSE is the root mean square of the fitting error in Eq. 19. c is the constant in $f(r_{ip})$ in Eq. 6

cal changes using association analysis between the mechanical parameters and histological scores. This study may aid clinical decision making on diagnosis of CD patients by relating measurable tissue stiffness parameters from in vivo distension tests to pathology changes.

4.2. Evaluation of intestinal stiffness at CD stenosis

Bowel stiffness is associated with wall deformability and intestinal motor function [22,28]. Changes in the wall stiffness induced by diseases reflect tissue remodeling [29-31] and may impair gut motility [29]. Previous studies from our group have shown associations between impaired bowel function and remodeled wall stiffness in patients with diabetes [29,30], systemic sclerosis [32] and irritable bowel syndrome [33,34]. Several stiffness indices have been proposed based on pressure-diameter relationships during bowel distension. These indices include distensibility index, compliance, and elastic modulus [9]. Several compression tests including strain elastography [11], micro-elastometer [12] or a multi-scale indenter [10] have been used to estimate the stiffness of CD intestinal strictures in humans. The studies demonstrated that the wall stiffness increased in regions with fibrotic changes. Strain elastography, micro-elastometer and indenter quantify tissue deformability, where the wall compression modulus was calculated from deformation and the applied press force within the organ. A softer region within the organ would display large changes in distance between the points, i.e., larger strains. However, the accuracy of the measurement depends on the distance from the organ to the transducer and the heterogeneity of the wall material [35,36]. Estimates of the wall stiffness from US imaging during distension provides quantitative information on both the configuration of a stenosis and the the morphometric change in the individual layers of the gut wall [18,37,38]. With the combined bag distension and ultrasound measurement in excised CD bowel segments, we measured morphometric parameters including wall thickness during distension at the stenotic site. Hence, the wall mechanical properties at the stenotic site can be assessed from the mechanical constants of the tissue. Compared with previous studies on CD stricture mechanical properties, we moved a step further by: 1) using intact segments, i.e. preserving the tissue structure and integrity during the test; 2) applying the three dimensional Demiray-type strain energy function model to describe the hyperelastic mechanical behavior of the stenotic small bowel, i.e. the non-linear, large deformation properties of the tissue stricture were assessed by the mechanical constants of the model; and 3) describing the association relationships between the mechanical remodeling and the pathological change of the tissue.

4.3. Grading the histological changes of the intestinal wall at CD stenosis

In order to analyze the association between bowel wall stiffness and the histological changes of the stenotic site, it was important

Table 3
Multiple regression analyses.

Main histological factors in intact wall				
Equation		F	*P*	Independent variables
AB = −4.048 - (0.225 * AL) + (0.329 * CI) + (0.468 * FB) + (0.0710 * MH)		6.789	0.003	AL 0.429 **CI 0.067** FB 0.101 MH 0.785
AB = −4.129 - (0.271 * AI+CI) + (0.515 * CI+FB) + (0.0545 * TP)		9.768	<0.001	AI + CI 0.687 **CI + FB 0.005** TP 0.079
Layer contributions				
	Equation	F	*P*	Independent variables
CI	AB = −3.333 + (0.873 * Mucosa) - (0.747 * Submucosa) + (0.936 * Muscle) + (0.363 * Adventitia)	5.104	0.009	**Mucosa 0.030** Submucosa 0.390 **Muscle 0.087** Adventitia 0.581
FB	AB = −0.940 - (0.00677 * Mucosa) + (0.344 * Submucosa) + (3.361 * Muscle) - (0.129 * Adventitia)	7.152	0.002	Mucosa 0.994 **Submucosa 0.011** **Muscle 0.022** Adventitia 0.868
CI + FB	AB = −4.206 + (0.589 * Mucosa) - (0.133 * Submucosa) + (0.739 * Muscle) + (0.0244 * Adventitia)	5.963	0.005	**Mucosa 0.066** **Submucosa 0.060** Muscle 0.790 Adventitia 0.946

Notes: Independent variables: p-values for the variables in the multiple regression equation.
Abbreviations: AB: Combined mechanical constants (a times b); AI: acute inflammation; CI: chronic inflammation; FB: fibrosis; MH: muscle hypertrophy; TP: total points; Bold items: indicating stronger dependency with AB

to use an appropriate method to grade the histological changes within the bowel wall. Measurement of histologic disease activity has potential value in CD. Most of the published histopathological characterization of Crohn's strictures were performed as part of radiological studies including US or CT with various histological grading schemes roughly assessing for inflammation and fibrosis [39-43]. Schaeffer et al [44] proposed a scoring system for semi-quantitative histological analysis of CD in surgical resection specimens to evaluate the changes related to anti-tumor necrosis factor therapy. More recently, Chen and co-workers also proposed a novel grading system for semi-quantitative histological analysis of CD in surgical resection specimens [6]. The latter has been developed as a comprehensive analysis of the histopathological elements in CD 'fibrostenosis' that covers not only inflammation and fibrosis but the full spectrum of inflammatory bowel disease pathology. Therefore, we adopted the methods from Chen et al [6] to grade inflammation, fibrosis, muscular hypertrophy and adipocyte proliferation in mucosa, submucosa, muscle and adventitia layers at stenosis site of CD bowel wall.

However, so far no validated histopathological scoring system is currently available for characterization of Crohn's bowel strictures [45-47]. Recently, De Voogd et al [46] systematically reviewed potential histological parameters that reflect either inflammation or fibrosis in strictures associated with CD. Their systematic review of sixteen studies may be the starting point for generating a robust, validated, reproducible and feasible histological scoring system by providing valuable information to consensus panels. More recently, Gordon et al [47] convened an expert panel to evaluate the appropriateness of histopathology scoring systems for CD small bowel strictures. In their work, a bowel wall stricture was histopathologically defined including the histopathological characteristics for active and chronic mucosal inflammatory diseases. The belief is that these consensus criteria for bowel stricture CD will standardize macro- and micro-pathological assessment, as well as inform development of a validated histopathology score system that can be used in clinical practice. However, for clinical practice a simpler or synthetic histopathological way to evaluate Crohn's bowel strictures may be needed. Knowledge may be gathered from analyses of assessment of histopathological scores for similar fibroproliferative diseases, such as liver fibrosis [48].

4.4. Intestinal wall stiffness and histological characteristics of the stenosis in CD

Clinically, CD is characterized by periods of remission and episodes of flare. Pathologically, CD is characterized by pronounced enteric connective tissue and inflammatory changes [49]. Long-lasting and recurring inflammation causes intestinal thickening, hardening and narrowing and, in turn stenosis [50]. CD patients with strictures are at risk for development of intestinal obstruction [51]. Theoretically, several histological changes may contribute to the bowel wall thickening and stricturing including fibrosis, hyperplasia of fat and/or smooth muscle tissues. Even edema as a part of inflammation may contribute. Tissue remodeling processes secondary to an excessive wound healing response are characterized by proliferation/differentiation of mesenchymal cells including fibroblasts, myofibroblasts and smooth muscle cells, and accumulation of excess extracellular matrix proteins [6]. When these changes occur in the bowel, wall thickening, and obstruction would be expected. Therefore, it is important to distinguish the histological changes. Especially, the fibrostenotics needs to be distinguished from inflammation-related bowel wall thickening because predominantly acute inflammatory stenosis may benefit from medical treatment. In contrast, fibrotic stenosis requires endoscopic balloon dilation or surgery [7].

In the present study, we found that the stiffness of the wall was most closely associated with chronic inflammation, fibrosis and the combination of the two. Analysis of layer contribution indicated

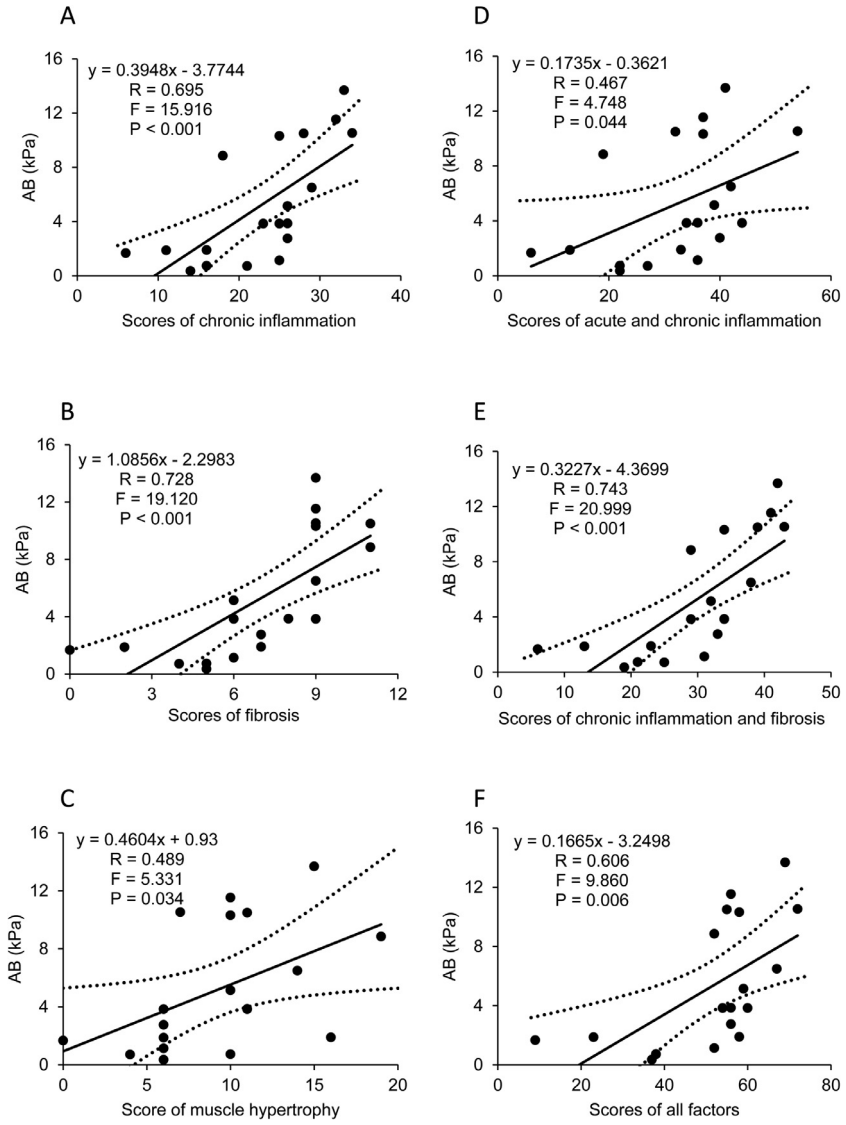

Fig. 4. The association between the combined material constant AB and scores of histological parameters from the intact wall. (A) chronic inflammation, (B) fibrosis, (C) muscular hypertrophy, (D) acute + chronic inflammation, (E) chronic inflammation + fibrosis, and (F) scores of all factors. The strongest positive association was found between the AB and chronic inflammation (A), fibrosis (B) and chronic inflammation + fibrosis (E). R, F and P values are presented in figures. The dotted lines are 95 % confidence intervals

that chronic inflammation in the mucosa layer and fibrosis in the submucosa and muscle layers contributed mostly to the wall stiffness. Thus, the more chronic inflammation and fibrosis, the stiffer bowel wall at a stenotic site. Our study demonstrated a strong relationship between the tissue stiffness and histological change of the tissue in CD strictures, i.e. the severer the disease, the stiffer wall of the CD stricture. The finding is consistent with the trend identified in previous compression studies on the bowel wall stiffness in CD patients [10-12]. However, it is difficult to compare the mechanical constants obtained in this study with the bowel wall stiffness in CD patient in previously published studies since different mechanical tests and mechanical models were used. Our results showed that biomechanical parameters potentially can be used as biomarkers to predict the pathological tissue change in CD patient, i.e. distension devices used in vivo may provide clinically useful diagnostic data for clinical decision making.

It is important to assess inflammation and fibrosis of CD bowel as they closely relate to patient treatment. Accurate evaluation of the extent and severity of inflammation and/or fibrosis in CD currently requires histopathological analysis of the bowel wall. However, in clinical practice and research, several non-histological methods are used to assess "inflammation" or "fibrosis" such as cross-sectional imaging including ultrasonography, CT and MRI [7,8,52-54]. These cross-sectional imaging techniques can quantitate prestenotic dilation, wall thickening and luminal narrowing. Hence, useful information can be obtained on the severity and extent of inflammation and fibrosis in CD disease [52,53].

4.5. Limitations of the study

In the present study, we only investigated the associations between stiffness and histological characteristics of bowel wall at stenotic site of CD at a single time point. The remodeling of small bowel stiffness during the development of the CD were not studied as function of time. Future studies need to access multiple sites including normal locations of bowel wall during CD progression in order to obtain more comprehensive data about the association between the development of the stiffness and histological characteristics. Furthermore, only 19 patients were included in the study. Despite the low number of subjects, we found associ-

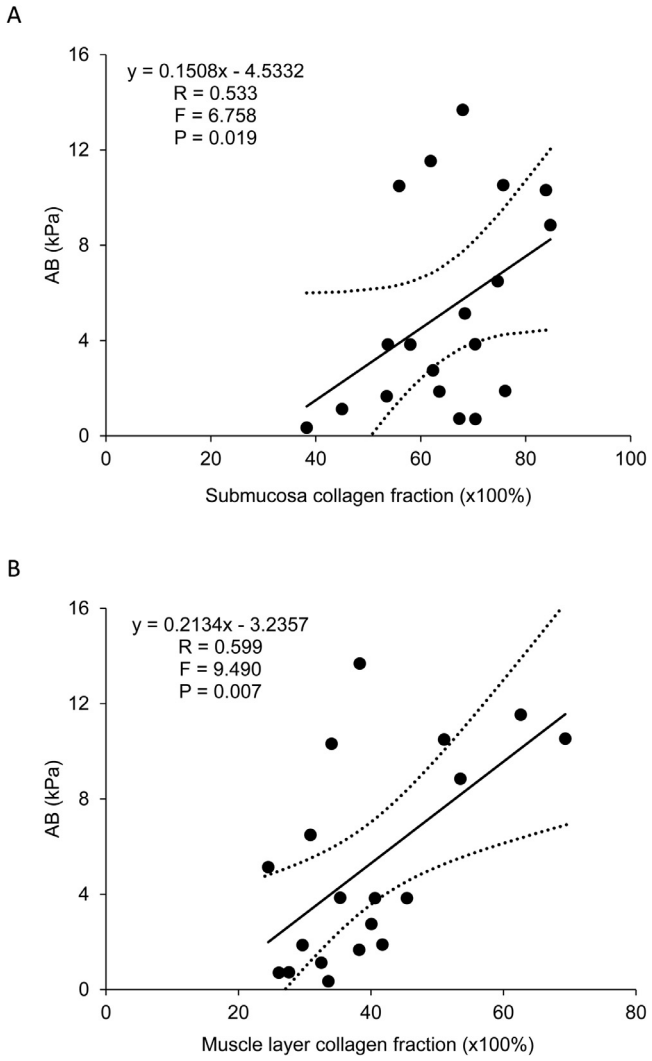

Fig. 5. Association between the combined material constant AB and fraction of collagen content. The linear regression analysis between the AB with collagen fraction in submucosa layer (A) and muscle layer (B) are shown. The AB was significantly associated with the collagen fraction in both the submucosa and muscle layers. R, F and P values are presented in figures. The dotted lines are 95 % confidence intervals.

ations between key parameters. These associations should be further explored in larger studies. In contrast to fibrotic tissue mechanical studies on liver [55], we used a step-wise distension protocol to study the small bowel distension properties and the time-dependent viscoelasticity of the tissue was not considered. Therefore, the mechanical constants could be underestimated in this study. This limitation can be overcome by adding viscoelasticity into the strain energy function and by conducting continuous ramp distension protocol in future studies. The applied histological score was not validated, and the individual scores were not weighted. Although we did not observe any acute tissue damage in the bowel wall after distension, minor (invisible) lesions may have occurred. However, such minor lesions would not affect the histology scores. Furthermore, although the histological analysis methods from Chen et al [6] to grade histological changes at stenosis site of CD bowel wall is comprehensive, such analyses may be too complicated to use in clinical practice. A simpler or synthetic way to distinguish between inflammation and fibrosis should be determined in future studies.

In this study, a bag with maximum diameter 30mm was used. The inner diameters of the small bowel at the stenotic location was $<$ 30mm at the highest distension pressure for all tissue samples. Hence, the bag pressure was identical to the pressure applied to the stenotic site. Since the dilated small bowel in adults can reach diameters exceeding 4cm [56], a bigger-sized bag would be needed for studying non-stenotic sites in future distensibility studies.

We assumed the diseased small bowel tissue as an incompressible (isovolumetric) solid material in this study. This is a reasonable assumption considering the high-water content in biological tissues and is based in a fact that the compression modulus of water is orders of magnitude larger than the distortional stiffness of tissues [57] and the pressures applied. In this study, all mechanical tests were done by submerging the tissue segment into an organ bath containing standard Krebs solution to maintain a completely hydrated state. Hence, there was no hydration related mechanical properties change during the test. The remodeled mechanical behavior of the small bowel in CD was described using mechanical constants from a three-dimensional, isotropic strain-energy function model. Although the model could quantify the stiffening of several soft biological tissues at high strains [15,16], the model cannot quantify the anisotropy of the tissue including the axial modulus. To explore tissue anisotropic mechanical properties, the fiber-reinforced anisotropic constitutive model developed by Holzapfel et al. [58] should be considered by integrating the collagenous component into the model.

5. Conclusions

We obtained quantitative measures of intestinal mechanical properties change in CD. Associations between the mechanical remodeling and histological characteristics were found in CD stenosis. The chronic inflammation and fibrosis are main contributors for the mechanical remodeling of the bowel wall. The histological characteristics in patients with CD can be predicted clinically by means of inflammation and fibrosis assessment in conjunction with tissue stiffness measurement.

Disclosure

We declare that we have no known competing financial interests or personal relationships that could have appeared to influence the work reported in this paper.

Declaration of Competing Interest

The authors declare that they have no known competing financial interests or personal relationships that could have appeared to influence the work reported in this paper.

Acknowledgements

This study was supported by the Karen Elise Jensen's Foundation (Grant No. 903959), and DL is partly supported by Steno Collaborative Grants 2018 from Novo Nordisk Fonden (Grant NNF18OC0052045).

We thank the surgeons Anders Tøttrup and Charlotte Buchard, Surgical Department P, Aarhus University Hospital, for recruitment of patients and surgical removal of bowel specimens for the majority of patients. We also would like to thank the dedicated nurses Margit Majgaard and Gitte Sørensen for assisting with the ex vivo biomechanical testing

Supplementary materials

Supplementary material associated with this article can be found, in the online version, at doi:10.1016/j.actbio.2021.06.011.

References

[1] M. Gajendran, P. Loganathan, A.P. Catinella, J.G. Hashash, A comprehensive review and update on Crohn's disease, Dis. Mon. 64 (2018) 20–57.
[2] B. Veauthier, J.R. Hornecker, Crohn's disease: diagnosis and management, Am. Fam. Physician. 98 (2018) 661–669.
[3] S. Aniwan, S.H. Park, E.V. Loftus Jr., Epidemiology, natural history, and risk stratification of Crohn's disease, Gastroenterol. Clin. North. Am. 46 (2017) 463–480.
[4] J. Torres, S. Mehandru, J.F. Colombel, L. Peyrin-Biroulet, Crohn's disease, Lancet 389 (2017) 1741–1755.
[5] W.P.W. Chan, F. Mourad, R.W. Leong, Crohn's disease associated strictures, J Gastroenterol. Hepatol. 33 (2018) 998–1008.
[6] W. Chen, C. Lu, C. Hirota, M. Iacucci, S. Ghosh, X. Gui, Smooth muscle hyperplasia/hypertrophy is the most prominent histological change in Crohn's fibrostenosing bowel strictures: a semiquantitative analysis by using a novel histological grading scheme, J. Crohns. Colitis. 11 (2017) 92–104.
[7] D. Bettenworth, A. Bokemeyer, M. Baker, R. Mao, C.E. Parker, T. Nguyen, C. Ma, J. Panés, J. Rimola, J.G. Fletcher, V. Jairath, B.G. Feagan, F. Rieder, Stenosis therapy and anti-fibrotic research (STAR) consortium. Assessment of Crohn's disease-associated small bowel strictures and fibrosis on cross-sectional imaging: a systematic review, Gut 68 (2019) 1115–1126.
[8] C. Lu, C. Merrill, A. Medellin, K. Novak, S.R. Wilson, Bowel ultrasound state of the art: grayscale and doppler ultrasound, contrast enhancement, and elastography in crohn disease, J. Ultrasound. Med. 38 (2019) 271–288.
[9] H. Gregersen, Biomechanics of the Gastrointestinal Tract - New Perspectives in Motility Research and Diagnostics, Springer-Verlag, London, 2002.
[10] R.W. Stidham, J. Xu, L.A. Johnson, K. Kim, D.S. Moons, B.J. McKenna, J.M. Rubin, P.D. Higgins, Ultrasound elasticity imaging for detecting intestinal fibrosis and inflammation in rats and humans with Crohn's disease, Gastroenterology 141 (2011) 819–826 e1.
[11] D.C. Stewart, D. Berrie, J. Li, X. Liu, C. Rickerson, D. Mkoji, A. Iqbal, S. Tan, A.L. Doty, S.C. Glover, C.S. Simmons, Quantitative assessment of intestinal stiffness and associations with fibrosis in human inflammatory bowel disease, PLoS One 13 (2018) e0200377.
[12] L.A. Johnson, E.S. Rodansky, K.L. Sauder, J.C. Horowitz, J.D. Mih, D.J. Tschumperlin, P.D. Higgins, Matrix stiffness corresponding to strictured bowel induces a fibrogenic response in human colonic fibroblasts, Inflamm. Bowel. Dis. 19 (2013) 891–903.
[13] R. Wilkens, R.H. Hagemann-Madsen, D.A. Peters, A.H. Nielsen, C.B. Nørager, H. Glerup, K. Krogh, Validity of contrast-enhanced ultrasonography and dynamic contrast-enhanced mr enterography in the assessment of transmural activity and fibrosis in Crohn's disease, J. Crohns. Colitis. 12 (2018) 48–56.
[14] L.E. Bailey, S.D. Ong, Krebs-Henseleit solution as a physiological buffer in perfused and superfused preparations, J. Pharmacol. Methods. 1 (1978) 171–175.
[15] H. Demiray, A note on the elasticity of soft biological tissues, J. Biomech. 5 (1972) 309–311.
[16] A. Delfino, N. Stergiopulos, J.E. Moore, J.J. Meister, Residual strain effects on the stress field in a thick wall finite element model of the human carotid bifurcation, J. Biomech. 30 (1997) 777–786.
[17] D. Liao, J. Zhao, H. Gregersen, 3d Mechanical properties of the partially obstructed guinea pig small intestine, J. Biomech. 43 (2010) 2079–2086.
[18] D. Liao, L. Hee, P. Sandager, N. Uldbjerg, H. Gregersen, Identification of biomechanical properties in vivo in human uterine cervix, J. Mech. Behav. Biomed. Mater. 39 (2014) 27–37.
[19] J.O. Clarke, N.K. Ahuja, N.Q. Fernandez-Becker, H. Gregersen, A.N. Kamal, A. Khan, K.L. Lynch, M.F. Vela, The functional lumen imaging probe in gastrointestinal disorders: the past, present, and future, Ann. N. Y. Acad. Sci. 1482 (2020) 16–25.
[20] E.N. Donnan, J.E. Pandolfino, Applying the functional luminal imaging probe to esophageal disorders, Curr. Gastroenterol. Rep. 22 (2020) 10.
[21] J.B. Frøkjaer, S.D. Andersen, S. Lundbye-Christensen, P. Funch-Jensen, A.M. Drewes, H. Gregersen, Sensation and distribution of stress and deformation in the human oesophagus, Neurogastroenterol. Motil. 18 (2006) 104–114.
[22] C. Gao, L. Arendt-Nielsen, W. Liu, P. Petersen, A.M. Drewes, H. Gregersen, Sensory and biomechanical responses to ramp-controlled distension of the human duodenum, Am. J. Physiol. Gastrointest. Liver. Physiol. 284 (2003) G461–G471.
[23] H. Gregersen, K.M. Lo, What is the future of impedance planimetry in gastroenterology? J. Neurogastroenterol. Motil. 24 (2018) 166–181.
[24] D.A.L. Hoff, B. McMahon, H. Gregersen, Esophageal multimodal stimulation and sensation, Ann. N. Y. Acad. Sci. 1434 (2018) 210–218.
[25] C. Lottrup, H. Gregersen, D. Liao, L. Fynne, J.B. Frøkjær, K. Krogh, J. Regan, P. Kunwald, B.P. McMahon, Functional lumen imaging of the gastrointestinal tract, J. Gastroenterol. 50 (2015) 1005–1016.
[26] J. Zhao, D. Liao, J. Yang, H. Gregersen, Biomechanical remodelling of obstructed guinea pig jejunum, J. Biomech. 43 (2010) 1322–1329.
[27] T.A. Zikos, G. Triadafilopoulos, J.O. Clarke, Esophagogastric junction outflow obstruction: current approach to diagnosis and management, Curr. Gastroenterol. Rep. 22 (2020) 9.
[28] P. Petersen, C. Gao, P. Rössel, P. Qvist, L. Arendt-Nielsen, H. Gregersen, A.M. Drewes, Sensory and biomechanical responses to distension of the normal human rectum and sigmoid colon, Digestion 64 (2001) 191–199.
[29] M. Zhao, D. Liao, J. Zhao, Diabetes-induced mechanophysiological changes in the small intestine and colon, World. J. Diabetes. 8 (2017) 249–269.
[30] J.B. Frokjaer, S.D. Andersen, N. Ejskjaer, P. Funch-Jensen, A.M. Drewes, H. Gregersen, Impaired contractility and remodeling of the upper gastrointestinal tract in diabetes mellitus type-1, World. J. Gastroenterol. 13 (2007) 4881–4890.
[31] M.J. Siegman, M. Eto, T.M. Butler, Remodeling of the rat distal colon in diabetes: function and ultrastructure, Am. J. Physiol. Cell. Physiol. 310 (2016) C151–C160.
[32] J. Pedersen, C. Gao, H. Egekvist, P. Bjerring, L. Arendt-Nielsen, H. Gregersen, A.M. Drewes, Pain and biomechanical responses to distention of the duodenum in patients with systemic sclerosis, Gastroenterology 124 (2003) 1230–1239.
[33] A.M. Drewes, P. Petersen, P. Rössel, C. Gao, J.B. Hansen, L. Arendt-Nielsen, Sensitivity and distensibility of the rectum and sigmoid colon in patients with irritable bowel syndrome, Scand. J. Gastroenterol 36 (2001) 827–832.
[34] J. Fassov, C. Brock, L. Lundby, A.M. Drewes, H. Gregersen, S. Buntzen, S. Laurberg, K. Krogh, Sacral nerve stimulation changes rectal sensitivity and biomechanical properties in patients with irritable bowel syndrome, Neurogastroenterol. Motil. 26 (2014) 1597–1604.
[35] E. Mazza, M. Parra-Saavedra, M. Bajka, E. Gratacos, K. Nicolaides, J. Deprest, In vivo assessment of the biomechanical properties of the uterine cervix in pregnancy, Prenat. Diagn. 34 (2014) 33–41.
[36] H. Gregersen, L. Hee, D. Liao, N. Uldbjerg, Distensibility and pain of the uterine cervix evaluated by novel techniques, Acta. Obstet. Gynecol. Scand. 95 (2016) 717–723.
[37] C. Lottrup, B.P. McMahon, P. Ejstrud, M.A. Ostapiuk, P. Funch-Jensen, A.M. Drewes, Esophagogastric junction distensibility in hiatus hernia, Dis. Esophagus. 29 (2016) 463–471.
[38] L. Hee, D. Liao, P. Sandager, H. Gregersen, N. Uldbjerg, Cervical stiffness evaluated in vivo by endoflip in pregnant women, PLoS. One. 9 (2014) e91121.
[39] M.V. Chiorean, K. Sandrasegaran, R. Saxena, D.D. Maglinte, A. Nakeeb, C.S. Johnson, Correlation of CT enteroclysis with surgical pathology in Crohn's disease, Am. J. Gastroenterol. 102 (2007) 2541–2550.
[40] N.R. Borley, N.J. Mortensen, D.P. Jewell, B.F. Warren, The relationship between inflammatory and serosal connective tissue changes in ileal Crohn's disease: evidence for a possible causative link, J. Pathol. 190 (2000) 196–202.
[41] L. Romanini, M. Passamonti, M. Navarria, F. Lanzarotto, V. Villanacci, L. Grazioli, F. Calliada, R. Maroldi, Quantitative analysis of contrast-enhanced ultrasonography of the bowel wall can predict disease activity in inflammatory bowel disease, Eur. J. Radiol. 83 (2014) 1317–1323.
[42] T. Sasaki, R. Kunisaki, H. Kinoshita, H. Kimura, T. Kodera, A. Nozawa, A. Hanzawa, N. Shibata, H. Yonezawa, E. Miyajima, S. Morita, S. Fujii, K. Numata, K. Tanaka, M. Tanaka, S. Maeda, Doppler ultrasound findings correlate with tissue vascularity and inflammation in surgical pathology specimens from patients with small intestinal Crohn's disease, BMC. Res. Notes. 7 (2014) 363.
[43] J. Rimola, N. Planell, S. Rodríguez, S. Delgado, I. Ordás, A. Ramírez-Morros, C. Ayuso, M. Aceituno, E. Ricart, A. Jauregui-Amezaga, J. Panés, M. Cuatrecasas, Characterization of inflammation and fibrosis in Crohn's disease lesions by magnetic resonance imaging, Am. J. Gastroenterol. 110 (2015) 432–440.
[44] D.F. Schaeffer, J.C. Walsh, R. Kirsch, M. Waterman, M.S. Silverberg, R.H. Riddell, Distinctive histopathologic phenotype in resection specimens from patients with Crohn's disease receiving anti-TNF-α therapy, Hum. Pathol. 45 (2014) 1928–1935.
[45] A. Mojtahed, R. Khanna, W.J. Sandborn, G.R. D'Haens, B.G. Feagan, L.M. Shackelton, K.A. Baker, E. Dubcenco, M.A. Valasek, K. Geboes, B.G. Levesque, Assessment of histologic disease activity in Crohn's disease: a systematic review, Inflamm. Bowel. Dis. 20 (2014) 2092–2103.
[46] F.A. De Voogd, A. Mookhoek, K.B. Gecse, G. De Hertogh, W.A. Bemelman, C.J. Buskens, G.R. D'Haens, Systematic Review: Histological Scoring of Strictures in Crohn's Disease, J. Crohns. Colitis. 14 (2020) 734–742.
[47] I.O. Gordon, D. Bettenworth, A. Bokemeyer, A. Srivastava, C. Rosty, G. de Hertogh, M.E. Robert, M.A. Valasek, R. Mao, J. Li, N. Harpaz, P. Borralho, R.K. Pai, R. Odze, R. Feakins, C.E. Parker, L. Guizzetti, T. Nguyen, L.M. Shackelton, W.J. Sandborn, V. Jairath, M. Baker, D. Bruining, J.G. Fletcher, B.G. Feagan, R.K. Pai, F. Rieder;, Stenosis Therapy and Anti-Fibrotic Research (STAR) Consortium, International consensus to standardise histopathological scoring for small bowel strictures in Crohn's disease, Gut. (2021 May 5) gutjnl-2021-324374. Epub ahead of print.
[48] N. Sato, A. Kenjo, A. Nishimagi, T. Kimura, R. Okada, T. Ishigame, Y. Kofunato, S. Yamada, Y. Hashimoto, S. Marubashi, Accuracy comparison of MR elastography and biological markers in detecting liver fibrosis and predicting postoperative ascites, HPB (Oxford) (2021 Feb 1) S1365-182X(21)00027-7. Epub ahead of print.
[49] D.C. Baumgart, W.J. Sandborn, Crohn's disease, Lancet 380 (2012) 1590–1605.
[50] J.B. Kirsner, Observations on the medical treatment of inflammatory bowel disease, JAMA 243 (1980) 557–564.
[51] L. Peyrin-Biroulet, W.S. Harmsen, W.J. Tremaine, A.R. Zinsmeister, W.J. Sandborn, E.V. Loftus Jr., Surgery in a population-based cohort of Crohn's disease from Olmsted County, Minnesota (1970-2004), Am. J. Gastroenterol. 107 (2012) 1693–1701.
[52] R. Gabbiadini, E. Zacharopoulou, F. Furfaro, V. Craviotto, A. Zilli, D. Gilardi, G. Roda, L. Loy, G. Fiorino, L. Peyrin-Biroulet, S. Danese, M. Allocca, Application of ultrasound elastography for assessing intestinal fibrosis in inflammatory bowel disease: fiction or reality? Curr. Drug. Targets. 22 (2021) 347–355.

[53] F. Ferretti, R. Cannatelli, S. Ardizzone, J.A. Maier, G. Maconi, Ultrasonographic evaluation of intestinal fibrosis and inflammation in Crohn's disease. The State of the Art, Front. Pharmacol. 12 (2021) 679924.
[54] G. Pellino, E. Nicolai, O.A. Catalano, S. Campione, F.P. D'Armiento, M. Salvatore, A. Cuocolo, F. Selvaggi, PET/MR versus PET/CT imaging: impact on the clinical management of small-bowel Crohn's disease, J. Crohns. Colitis. 10 (2016) 277–285.
[55] M. Perepelyuk, L. Chin, X. Cao, A. van Oosten, V.B. Shenoy, P.A. Janmey, R.G. Wells, Normal and fibrotic rat livers demonstrate shear strain softening and compression stiffening: a model for soft tissue mechanics, PLoS One 11 (2016) e0146588.
[56] S.L. Jacobs, A. Rozenblit, Z. Ricci, J. Roberts, D. Milikow, V. Chernyak, E. Wolf, Small bowel faeces sign in patients without small bowel obstruction, Clin. Radiol. 62 (2007) 353–357.
[57] A.E. Ehret, K. Bircher, A. Stracuzzi, V. Marina, M. Zündel, E. Mazza, Inverse poroelasticity as a fundamental mechanism in biomechanics and mechanobiology, Nat. Commun. 8 (2017) 1002.
[58] A.H. Gerhard, C.G. Thomas, W.O. Ray, A new constitutive framework for arterial wall mechanics and a comparative study of material models, J. Elast. Phys. Sci. Solids 61 (2000) 1–48.